Low-Altitude Platform to Enhance Communications Reliability in Disaster Environments

Sateaa H. Alnajjar
Universiti Malaysia Perlis (UniMAP)/ School of Computer and Communication Engineering,
Email: h.sat.nj@gmail

Fareq Malek, Mohd S. Razalli and Mohd S. Ahmad
Universiti Malaysia Perlis /School of Electrical System Engineering[2, 4] and School of Computer and Communication Engineering[3], Malaysia
Email: mfareq@unimap.edu.my

Abstract— **Natural disasters can cause a massive damage of life and property. Mobile communications technologies can be used to reduce the effect of disaster in isolated areas. The approach which has been adopted throughout this study by utilizes a Low-altitude Platform system (L-APs) as a technique to enhance the performance of communications network. However, the proposed approach was accompanied by some challenges, i.e. Instability of communication systems Inside-platform; and the needed to improve the quality of service (QoS). These challenges hinder network node for deployment. The situation led to creation a smart communication platform system (SCPS) base station. This system has characterized by the ability to adjustment with external factors that prevent stabilization. Moreover, SCPS has provisioned QoS via hybrid Free-Space Optics/radio Frequency (FSO/RF) networks as a technique to improve data propagation to the "last mile." A new method is used to connect several aerial platforms that are helpful in increasing the range of the network deployment. Therefore, the purpose of this study is to examine the performance of these platforms in various weather environments.**

Index Terms—— **low-altitude platform system, free space optic, mobile platforms, communication Network, and disaster area.**

I. Introduction

The Asia-Pacific Disaster Report devoted an entire section to a new technology and the way it can be used to enhance disaster risk management [1]. Pacific Nations began to focus on "The role of communication to reduce the impact of disasters," particularly after the recent events.

Where the traditional methods are ineffective to resolving these difficulties, the communication systems using balloons over the ground were suggested to enhance a communication backbone in natural disasters [2]. Low Altitude Platform (LAP) is used as an alternative solution to emergency communication systems [3]. The researchers of Niigata-Japan University offered a constructive study which investigates the statistical characteristics of the wireless channel [4].

However, vibration on a platform due to the wind is considered, one of the critical points that effected on a platform performance. The approach which is adopted in this study works by utilizing an LAP as a technique to enhance the performance of communication network. However, suggestion still faces certain challenges, which require an effective solution. To be more specific, these challenges include the constraints confronted by a network deployment via the instability of communication systems in the inter-platform in addition to the requirements for enhancing the quality of service. In fact, there is a correlation between these restrictions. A Free-Space Optic (FSO) communication links offer a probability of enhanced high data rate communication between nodes' deployment. However, these have a narrow beam divergence and need to steer laser beams in free-space between bi-directional FSO systems. These conceptualizations demand establishing a stand-alone smart platform that uses free-space optics as a technique to connect the network nodes. This platform is a base station which is characterized by the ability to adjust to external factors that prevent stabilization, in order to maintain a line-of-sight (LoS) propagation. However, a new approach is used to connect several aerial platforms at multi-levels to deploy network nodes with terrestrial remote-sensing. The purpose of this study is to develop a communication platform in low-altitude to overcome the restrictions. The paper's aims are to: 1) Linked aerial platforms in low attitude at Multi-levels of deployments. In addition to that, it aims at distributing a high- QoS to the End-System for enhancement the reliability of data propagation, by establishing free space optical links between mobile platforms. 2) Guide signal between network's nodes with acceptable BER.

doi:10.4304/jait.5.1.21-30

This requires creating a control system to maintain LoS path between bi-directional FSO. 3) Evaluate the SCPS performance at different environmental conditions. This paper is organized as follows. Section 2, demonstrates the structure of the network. Section 3, divided into two parts: first describes the methodology of controlling system, and the second focused on FSO design. The experimental results in this paper presented in section 4. Finally, research summary is in the latter part.

II. Network Architecture

Figure1demonstrations the correlation between the two levels of deployment. This study examines the process of data transmission between each of the communication and surveillance equipment's that are installed on the L-AP, as well as those installed on the ground. Depending on the region's requirement attitude it will demonstrate the main scenario for evaluation purposes. Suggested scenario uses two aerial platforms for adaption with ground station .i.e., Sky station1 (S^{S1}), which serves as the root node (RN) and is located within the first-level nodes (1^{L}Ns) of network deployment, and the second node (2^{nd}N) sky station two (S^{S2}) to receive the signal transmitted by the RN.

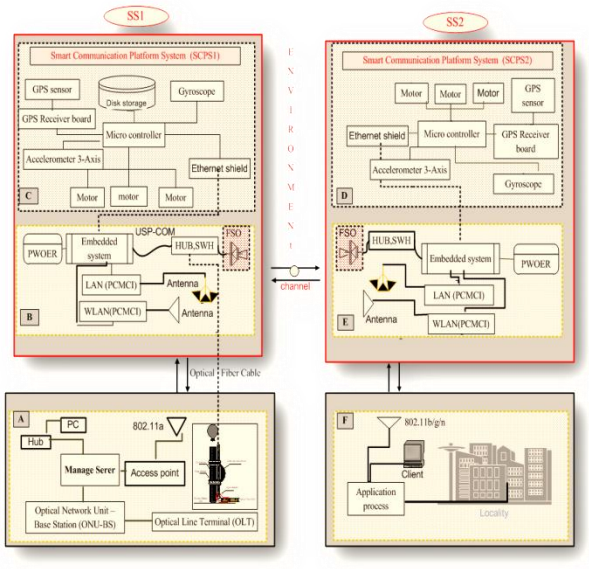

Figure1. Structure of the network design

Methodology for signal transmission between nodes used the following approach:

1) Radio frequency (RF) cycle: RN via the IEEE 802.11a is connected to the ground station (GS) .In second phase, the RN is linked to the 2^{nd}N through RF, and all nods provide coverage area to the ground by utilizing the IEEE802.11.b/g/n standard.
2) Optical cycle: the GS is connected to S^{S1} through a fiber-optic cable and RN is connected to 2^{nd}N - S^{S2} via FSO channel to increase the quality of service. Multiple-level architecture needs a guidance control system to keep the line of sight between a node's deployments to ensure data packets can reach the desired destination.

Smart communication platform system (SCPS) has been used in each network nodes, which is characterized being a light-weight, low cost, and it's able to sensing external environment. The system aims to stabilize communications systems and consists of two main units, i.e.; control system and communications unit. Figure 2 describes signal transfer mechanism between the two nodes with major components of the control system inside SCPS.

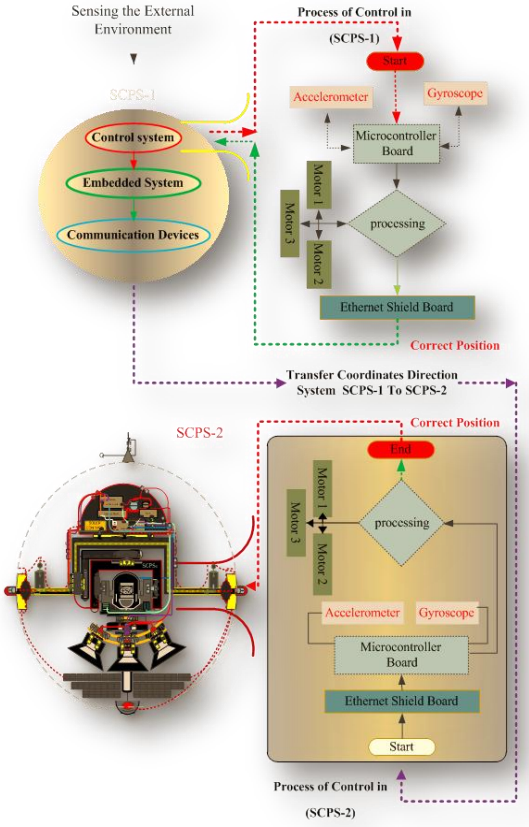

Figuare2. Sensing and control mechanism in SCPS

The accelerometer in algorithm that appears in figure 2 is to measures the acceleration resulting from an external force vector, in addition to tracking these changes in motion. This characteristic can be used to transfer body coordinates in sync with the movement. This study focuses on the issue of sensing the movement angle changes in order to find the appropriate means to modify the position of the body. The gyroscope is to measure the rate of changes in the angle of deviation about a reference point. This point is an important aspect of the stability of the system. To clarify the situation, it will review the procedures that used to address the change in the ratio of an angle. It can briefly review the sensor function based on the MEMS (Micro-Electro-Mechanical Systems) algorithm. Let a vector (R) represent the coordinates of the SCPS, i.e., Rcs x, Rcs y and Rcs z, which are the

projections of the R vector onto the X, Y, and Z axes, respectively and let the control system(cs) represent the control system inside the platform.

The Pythagorean Theorem in 3-dimensions can be stated as follows:

$$Rcs2 = Rcsx2 + Rcsy2 + RcsZ2 \quad (1)$$

Figure 3.5 shows the position of the R-vector at 45 degrees toward the XZ plane. Inertial forces (I) on the three axes are X=0.707g; Y=0g; Z= -0.707g, note that $0.707 = \sqrt{\frac{1}{2}}$ this value is included in the equation above.

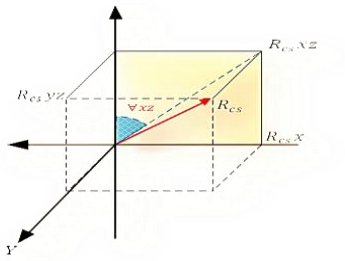

Figure3. Geometric Description of the Vector Coordinates

Using the fact that the force of gravity equals 1g = 9.8m/s^2, the Eq.1 can be formulated as follows:

$$12 = (-\sqrt{\tfrac{1}{2}})2 + 0 + (-\sqrt{\tfrac{1}{2}})2 \quad (2)$$

Comparing the equation above with Equation (3.1) yields

$$Rcs = 1, Rcsx = (-\sqrt{\tfrac{1}{2}}), Rcsy = 0, Rcsz = (-\sqrt{\tfrac{1}{2}}) \quad (3)$$

The 1-axis gyroscope can measure the rotation around one direction. $Rcs\ xz$ is the projection of the inertial force vector Rcs on the XZ plane. The ($\forall$xz) is the angle between the Rcs xz vector and Z plane and can be derived by using the formula above, therefore can it get:

$$Rcs\ xz2 = Rcs\ x2 + Rcs\ Z2 \quad (4)$$

This describes the change that occurred in angle ($\forall$xz), and the gyro measures the rate of ($\forall$xz) changes. In simple terms, the Gyro value output is linearly related to the rate of $\forall$xz change. To clarify the changing rate concept, let us assume the need to measure the rotation angles at time zero (T0) and that $\forall$xz is defined as Axz0 while (T1) measures $\forall$xz once more.

$$\text{The Rate of } \forall xz = \frac{(\forall xz1 - \forall xz0)}{(T1 - T0)} \quad (5)$$

The angle of $\forall$xz is in degrees and the time in seconds. The rate of $\forall$xz will, then, be expressed in deg /sec. In practice, the outcome of the gyroscope value can be obtained by the use of the sensor-specifications which are as follows: an ADC (analogue to digital converter) with a 10-bit module with an output value in the range of (0 to 1023); A reference voltage (V_{ref}) of 3.3V; a sensitivity value (Sv) expressed in (mV/deg/sec) and zero rate-voltage at 1.23V. Note that the value of zero-voltage represents the attitude of the gyro when it is constant and not subject to any motion, so the rate of the angle of interest can be found as follows:

$$Rate\ of, \forall xz = \frac{\frac{(ADC\ Rcs\ x\ z\ Vref)}{output\ range\ value\ (1023) - Vzero\ rate}}{Sv} \quad (6)$$

The coordinates of the SCPS's position are sent to the gyroscope to be rotated according to any change in the orientation of the rotation axis for a SCPS body. After the gyroscope output data is processed by the micro controller, the signal is sent to the motors to correct the direction of the SCPS. To interpret the external movement data, (C) programming language was used to convey the signal from the sensing system to a micro-controller. Figure3 describes the way the mechanism can be controlled with the main components of the system. Assembling these components in one unit creates a smart communication platform system. The orientation and control of the system with its structural infrastructure are applied to the rest of network platforms. On the other, communication unite composed of i.e. 1) a Global Positioning System (GPS), that provides reliable location and time information for the SCPS; 2) Embedded system hardware, and a personal computer memory card international (PCMCIA)–WAN and LAN, in addition to the FSO system .3) All of these components have been installed on the dynamic parts of the platform that include three motors, which are designed to receive the signal from the micro-controller. 4) The three-axis gyroscope is to measures the rate of change in the deviation angle about a reference point, for further information about SCPS [5-6].

III. Research Methodology

The study focused on platform performance and the ability to address the external factors which effect on system stability

A. SCPS Control system Design

The objective of SCPS control system is to achieve stabilization, since vibration and random movements, due to the external environment influences, lead to communication loss between node's deployments.

SCPS employs close-loop control to terminate this kind of motion. There are three PI-controllers, and each unit is used for each gimbals'-servo motor, This procedure assistances to ensure that zero state errors occur in step reference commands, as well as, will provide control over the bandwidth of the closed-loop system. There are three servomotors, one for each loop, and a Gimbals' - motor driver is used to moving the SCPS to a new reference point. In addition, it compensates the disturbance that occurs in the platform. Figure 4

illustrates the close-loop that is used in SCPS unit.

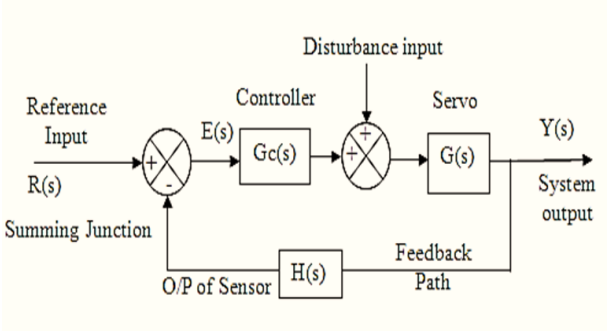

Figure 4.SCPS -Feedback Controller Loop for Each Axis

In this research, a PI controller is applied in order to achieve high control system performance. The tracking error E(s) for a closed loop control system shown in Figure. 4 can be defined as:

$$E(s) = R(s)-Y(s) \quad (4)$$

Where R(s) is the input signal and the Y(s) is the system output. For unity feedback system the output signal Y(s) can be defined as:

$$Y(s) = Gc(s)\,G(s) / (1+ Gc(s)\,G(s)\,H(s)), R(s)$$

$$+ G(s)/ (1+ Gc(s)\,G(s)\,H(s)), D(S) \quad (5)$$

Where G(s) is the DC servomotor transfer function, Gc(s) is the controller transfer function; H(S) is a sensor transfer function; D(s) is the disturbance signals.

Proportional- Integral- Derivative **(**PID) tuner computes the responses of the closed-loop depends on the input disturbance rejection function *d* changing from *r* to *y* as clarified in Figure 5, and this concept is defined as:

$$G(s)/ (1+Gc(s)\,G(s)) \quad (6)$$

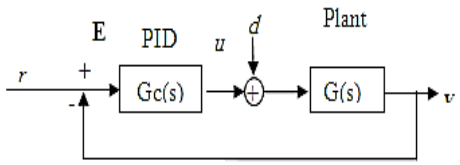

Figure5. Disturbance Rejection Function From (r to y)

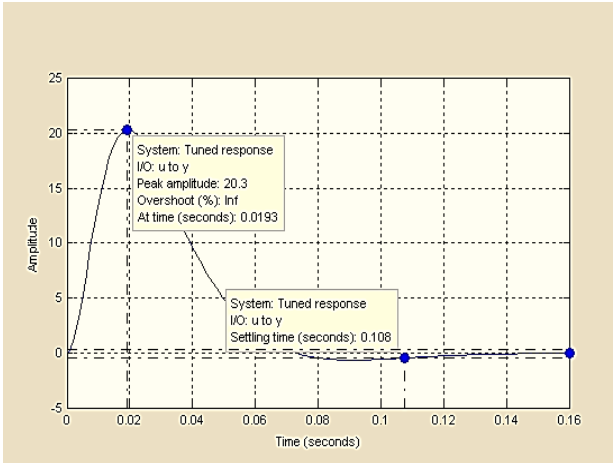

Figure6. Response Curve for Input Disturbance Rejection

The close loop system in Figure 6, displays the system response to the disturbance loading (a disturbance which is in the plant input).The disturbance peak amplitude is 20.3 at 0.0193 sec, thus, it can obtain a settling time at 0.108 sec to reach the steady-state output for *y* in response to a unit step disturbance input *d* at a 0.16 sec.

The output of disturbance rejection input is clarified in Figure 7. The Procedure that is employed in system design is used in cases which require the rejection of the disturbances. For evaluating the stability of SCPS, we should recall the close-loop control system, according to [7] "which a feedback control system could be stable if all the roots with their characteristic transfer function have negative real parts, i.e. at the left side of imaginary axis.

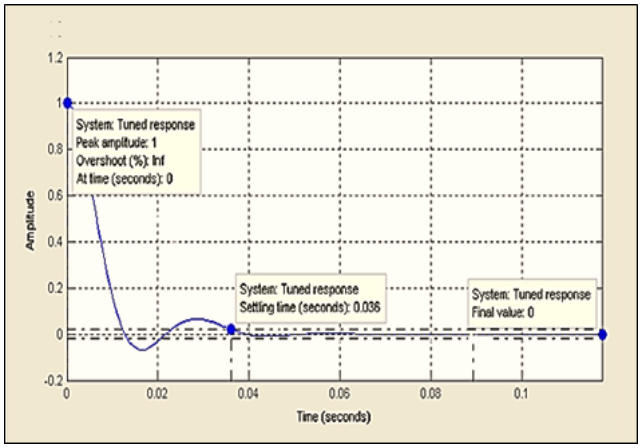

Figure7. Response Curve for Output Disturbance Rejection

However, if any root of the close-loop transfer function is on or at the right side of the imaginary axis, it becomes unstable". Through this rule, the concept of system stability can be clarified. Based on the minimization of integral of time-weighted absolute error, a robust proportional-integral (PI) controller is designed to achieve high performance and high stabilization precision for the LoS stabilization system.

Figure8 Illustrate the pole–zero map for close-loop control system that uses a tool preferences editor in linear

time invariant (LTI) function to compare the response plots of signal input- signal output (SISO) design task in MATLAB environment .The diagram shown in figure 7.

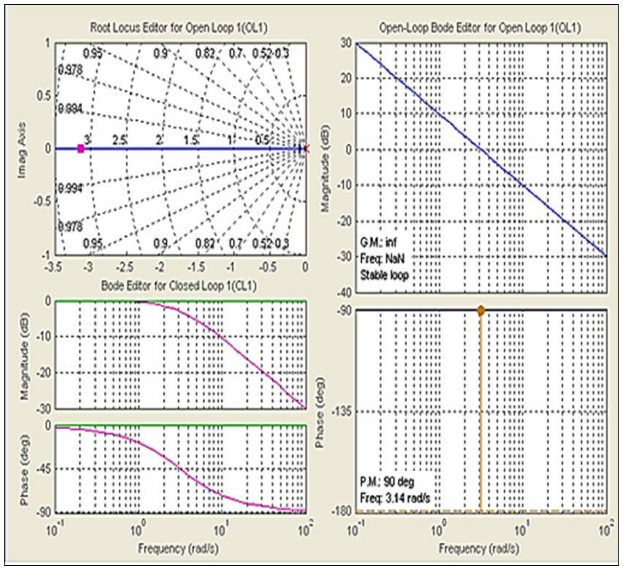

(A)

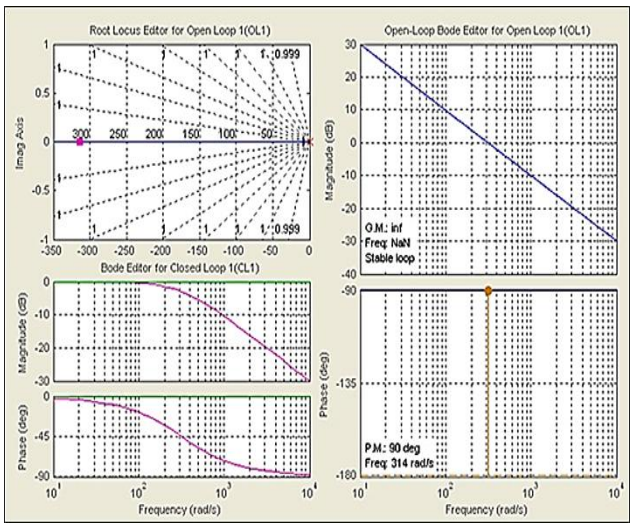

(B)

Figure8. Poles of Closed-Loop

Indicates the poles of closed-loop in location (-3.1) at 3.14 rad/sec bandwidth. A feedback control system could be stable if all the roots with their characteristic transfer function have negative real parts, i.e. at the left of imaginary axis. The red boxes in the Root Locus plot represent the closed-loop poles for the gain value that is specified in the current compensator pane. Open-loop Bode diagram that appears in the right side of Figure 8 demonstrations magnitude and phase plots for SCPS system. This curve displays the Bode phase response of the open-loop system at phase margin (P.M) 90 deg and frequency 3.14 rad/sec. The plot diagram that appears in the lower left side of the figure 8 displays the Bode magnitude response of the closed-loop system, the bode diagram computes the logarithmic gain and phase angles of the closed-loop frequency response from command reference input to output theta "θ". Figure 8 part (B) shows the same specification that is explained in Figure 8 part (A) with a frequency of 314 rad/sec. The purpose of this testing is to demonstrate the effectiveness of performance in the low and high ranges of frequencies. Furthermore it is clear that the system response is located on the left side of the imaginary area, this is a proof that the system is stable, based on the condition that is supposed by the previous definition.

In order to verify the effectiveness of the performance, will be creating an artificial motion on the system for measuring disturbance that occurs in the platform. The SimMechanics pendulum model used to generate this kind of movement on the SCPS.

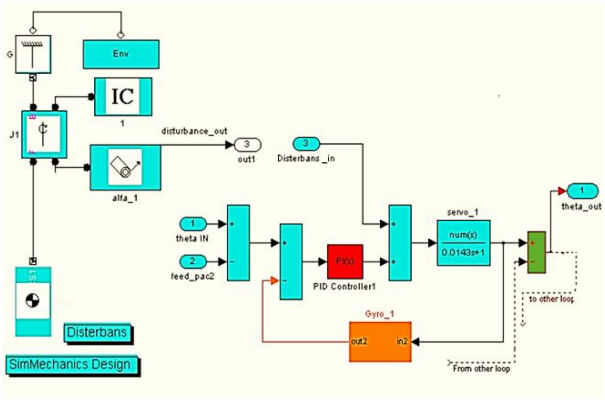

Figure 9.SCPS -Feedback Controller Loop for Each Axis

The design of the pendulum is shown on the left side of Figure 9, indicates the sub-system model, which is connected with SCPS-close loop model to create disturbance state on the system.

B. Free Space Optics System Design

In order to examine the FSO performance, it is necessary to take some of the system parameters into consideration. Generally, these factors can be divided into two different categories:

The first category is the internal parameters related to the FSO design, i.e., including optic power, bandwidth transmission, divergence angle, optical loss on transmission side and bit error rate in a receiver field of view (FOV) on the receive side. As for the second which is external limitation, FSO channel may lead to signal loss and link failure as a result of atmospheric attenuation. The Beers-Lambert law represents the relation between the powers of the transmitted signal and the received signal in the presence of atmospheric attenuation [8],

$$P_R = P_T \exp(-\sigma Z) \quad (7)$$

Where "P_T, P_R" stand for the transmitted and received power respectively, "σ" represents the atmospheric attenuation coefficient, "Z" is the connection rang.The bi-directional FSO transmission and receiving system require a fundamental prerequisite, i.e., a line of view for both sides.The wireless optical beam is commonly used

for establishing a data bridge between two remote network nodes and is more suited to high-bandwidth applications. To estimate the enhancement of the guidance system platforms requires evaluating the performance of the inter-platform communications system. Concepts and devices which are used in bi-directional FSO, (this design is described in figure 10.) utilize an optical simulator software "*Optisystem*™".

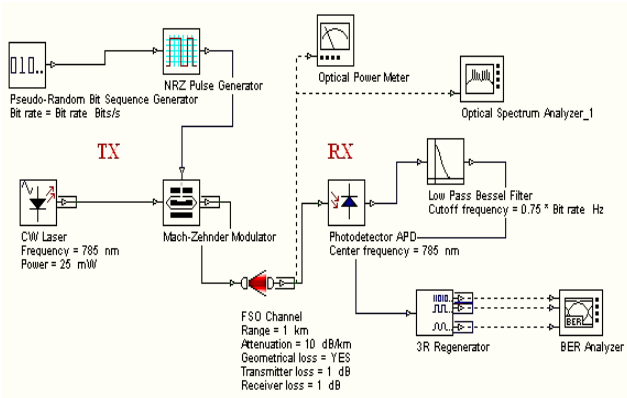

Figure10. Initial Design of Bi-Directional FSO Transmission Channel

The design represents a transmitter side in the RN, while the receipt is shown in the 2ndN.The transmission part of FSO entire-SCPS1 includes a pseudo-random bit generator, a non-return-to-zero (NRZ) pulse generator, continuous wave (CW) laser diodes, and a Mach-Zehnder Modulator. While the avalanche photodiode (APD) and the low-pass Gaussian filter are used in the receiver part of a S^{S2} propagate. The parameters of the FSO system are set according to the typical industry values in order to simulate a real-world environment as closely as possible. Table 1 indicates the parameters that have been used in FSO channel configuration. The performance test is continued by changing the FSO channel configuration until an unacceptable BER is obtained.

TABLE.1.
FSO CHANNEL CONFIGURATION.

CHANNEL CONFLAGRATION	PARAMETER
Range	1000-4000 m
Attenuation Rang	3-10 db/km
Transmitter- Loss	1dB
Receive- Loss	1dB
Transmission Power	25 mW
Frequency	785 nm
Beam Divergences	1 mrad

IV. EXPERIMENTAL RESULTS

This part will evaluate the performance of the platform stabilization to ensure LoS propagation between the transmitter sides. The other part will show the performance of the communication system that is installed inside the platform as well as comparing the results of the efficiency of the transmission channel.

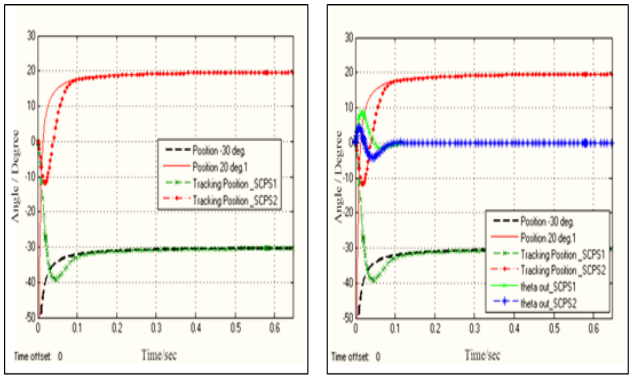

(A) (B)

Figure11. Behavior of the Systems

To determine the system response and its resistance to the changes in direction of a platform, the angle is set in initial examination to be nearly identical to changes of SCPS direction. In fact, platform changes are due to the external influences that cause vibration of a platform. The procedures to assess the system performance are as follows, i.e. the attitude of RN_SCPSv1 at "-30" degrees (deg) while position of 2ndN_SCPS2 is at "20"deg. Figure 11 (A) shows the status of tracking the deviation angle that has entered the systems. Figure 11 (B) which is shown as stability case illustrates how the SCPS modules reduce the gap between its current location and the successive deviation angles. Recent results indicate that the line of sight between network nodes has been achieved.

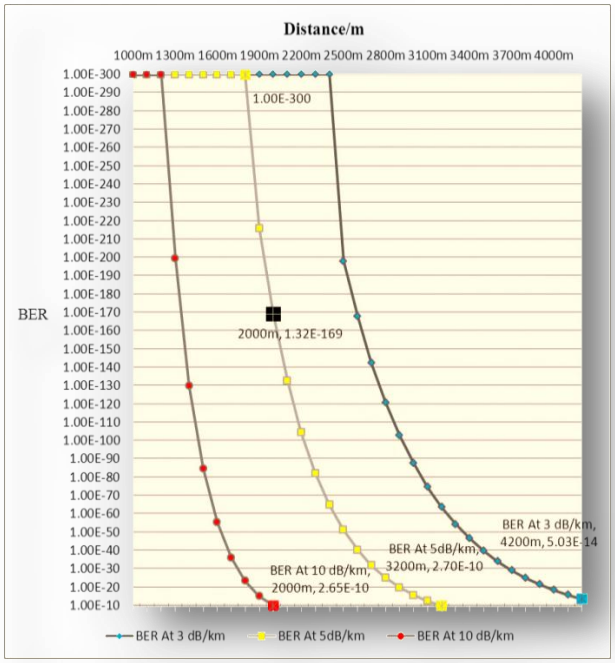

Figure12. Effective Link Range vs. Weather Coefficient at 3, 5 and 10 (dB/km)

The second results part explains in detail the efficiency of communication within the systems platform. Figure 12 shows the correlation between attenuation at different weather conditions vs. minimum BER at a distance of 2000 m. The curve in Figure 12 illustrates a three essential point, which represent the attenuation coefficient in different cases, i.e., in clear air it is 3 dB/km = Light rain (5-10 millimeter /hour) - Light haze; 5 dB/km = Light to medium rain (15-20 mm/hr) – Haze; 10 dB/km = Medium to heavy rain (45 mm/hr) - Light snow - Thin fog [9]. The previous result is suitable for attenuation less than 10 (dB /km), but inappropriate in case of heavy rain or fog. This defect is considered an obstruction in case of network deployment in such environmental conditions, specifically in case of FSO as a transmitter between the GU and the SCPS at less than 1000m altitude.

The reasons for this customization are that climate challenges are usually the toughest in levels close to the ground and their impact begins a downward course at high altitudes.

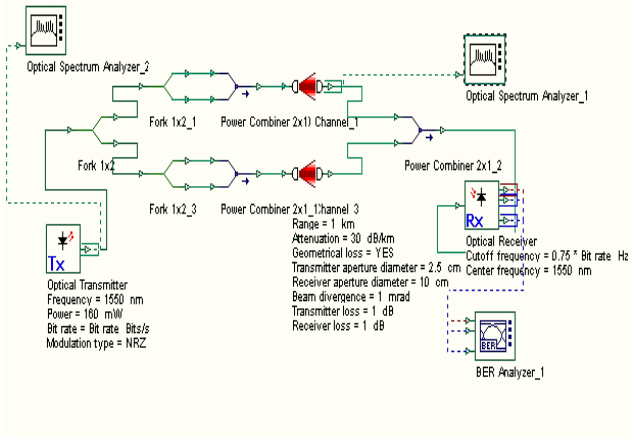

Figure13. Multiple FSO Transmission Channels

The previous negative situation has led to unacceptable BER. Therefore, to increase the efficiency of architecture of bi-directional FSO system, multiple channels transmission is used to improve the quality of an FSO. Accordingly, simulation design of the multiple higher laser beam channels at 320 mW peak (2 x 160 mW) with 10 cm diameters receive aperture. High-powered laser transmitters are able to penetrate heavy rain, snow and fog far more effectively and consistently. According to [9] Medium snow - Light fog @30 dB/km = Rain (up to 180 mm/hr) - Blizzard - Moderate fog. In order to obtain final results, Figure 13 illustrates the FSO system topology via utilizing multiple high-powered strengthen transmitters to increase data transmission reliability over the extreme environmental situations.

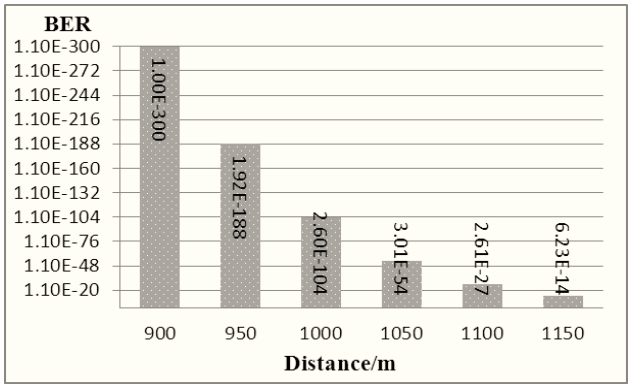

Figure14. Correlation between Distances vs. BER at (30 dB/km) Attenuation

Figure 14 shows the correlation between attenuation at 30 (dB/km) vs. minimum (Min) BET to a range of distances close to 1000m. The results show the efficiency of the system to accommodate the increase in attenuation coefficients. This is proof that the system in overcoming the problem of high rate of an attenuation coefficient.

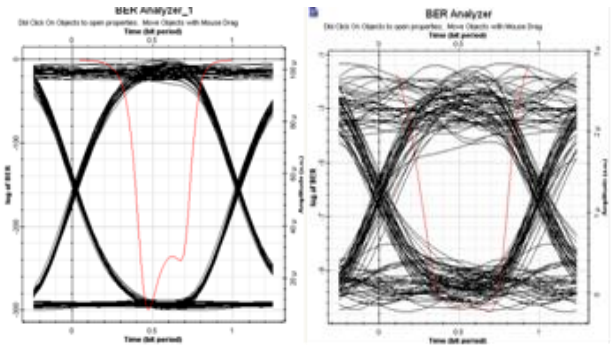

(A) (B)

Figure15. Min BER at 10 (dB/km) Weather Coefficients

Figures 15(A) and (B), illustrate the distortion in eye diagram utilizing BER analyzer to evaluate the attenuation coefficient. Figures 15(A) illustrate the Min BER becomes approximately 5.32327E-102 at 10 dB/km over a distance up to 2000m, comparing these results with the initial design is shown in figure 15 (B) proves that BER is up to 2.65E-10 through the distance of 2000m at an identical rate of "10 dB/km" attenuation, according to Figure 11results. Knowing that minimum acceptable BER is 1.E-9 [10].

A. Verification for Achieving LoS

In order to verify the performance of bi-directional FSO system, we must ensure from SCPS- control system's ability to overcome constraints that are imposed by the narrow beam. The subsequent procedure includes the most important measures that have been used in the multiple-characteristics test. These actions can be summarized as stated below.

In fact, the first stage requires evaluation systems that can identify the system’s reaction to each direction change and analyze the response to evaluate the system’s effectiveness. A pendulum motion model in the

MATLAB SimMechanics environment was used to generate the complex, unbalanced situation state in the SCPS units.

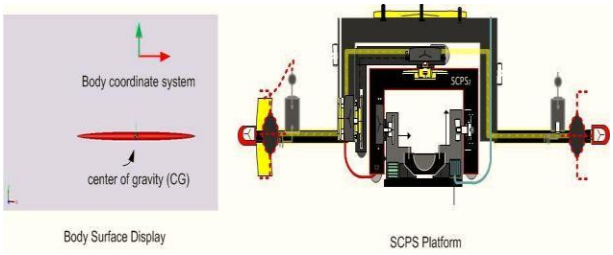

(A)

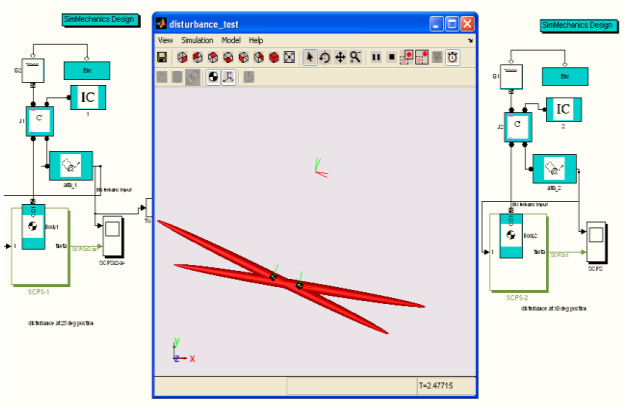

(B)

Figure16. (A) Exemplification of the Platform Format on MATLAB , (B) Procedures Implementations for Sending and Receiving Signal between the Two Systems

Figure 16(A) Exemplification of the Platform Format on MATLAB Environment. Figure 16(B) illustrates process of linking the SCPS-control system in both nodes with SimMechanics pendulum models. The pictures in the middle form display a platform during execution, which clearly shows the difference between the coordinates of the two nodes, deviation in the platform-coordinates is the result of entry commands to simulation program.

Figures 17 show the unbalanced situation with systems response. System coordinates in the initial phase were at an angle half-theta 1/2 θ = ± 30º along the line of view between the two nodes, and the angle was created to represent the coordinates' changes in the direction of SCPS-S^{S1} deviation from the LoS attitude. On the remote side, SCPS-S^{S2} arranged based on the 1/2 θ = ± 10º.

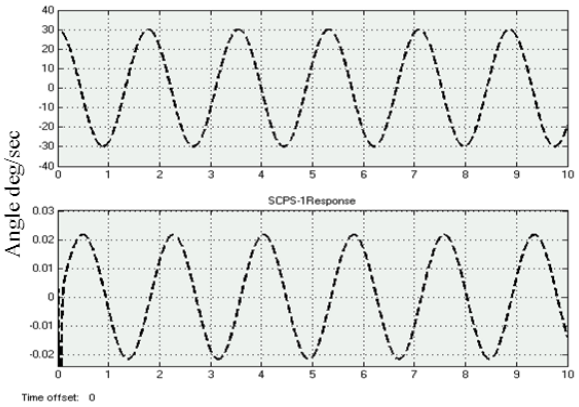

(A)

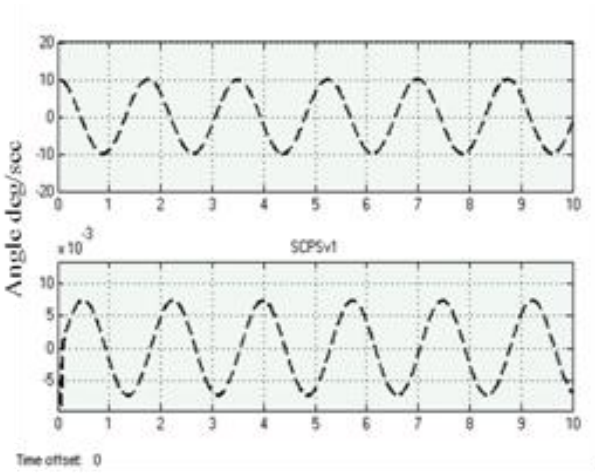

(B)

Figure17. (A) Disturbance and response on the SCPS-S^{S1}, and (B) illustrate the same procedure in (remote side) SCPS-S^{S2}.

Figure 17(A) shows how the SCPS reduces the gap between its current location and the successive deviation angles. System limits response will be ± 1/2 θ = 0.0208º.

Figure 17(B) shows the receiving remote side of the FSO system, the response approximately is ± 1/2 θ = 0.007 º.

The FSO system has a narrow laser beam. This property should be combined with the system response, to make sure the response did not exceed the maximum acceptance angle 8.5 mrad in FSO reserve side, according to product specification.

Figure 18 demonstrates a comprehensive manner of the systems attitude, specifically bi-directional FSO within each platform. Current vibrations exist for each platform, which, in fact, adversely affect the beam deflection angle to the LoS. The curve on the left side of Figure 17 represents the FSO transmitter system in SCPS-S^{S1}, and it demonstrates the maximum and minimum threshold vibrations. The limits of vibrations are represented by angles of +½ θ ≈ 0.0208 and - ½ θ) ≈ 0.020 °, respectively. The right side shows the receiver FSO side in SCPS-S^{S2}. The displacement of the (FSO-lens) limits represents an angle between +½ θ ≈ 0.00726°

and -½ θ ≈ -0.00731 °. The maximum acceptance angle has been appeared on the figure sideline, to compare the respond of systems with the permissible limits.

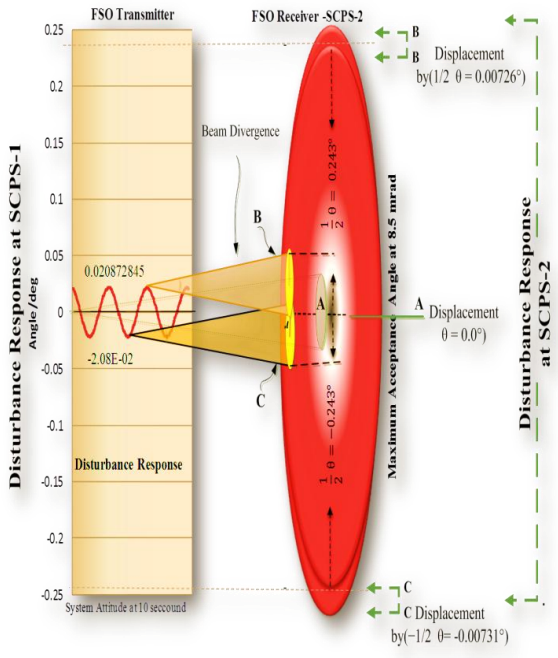

Figure18. Line-of-sight between the two systems

In order to analyze the results in more depth, three cases can be used to represent the beam divergence angle, as follows:

Case 1: It represents the zero case signified by (A) point, and the spot of (A) proceed describes the laser beam projections on the FSO receiver lens.

Case 2: Displacement that occurs in angle value of beam divergence, which is equivalent to the quantity of the maximum threshold vibrations, this condition has been signified by (B) point. The upper limit for a response system was performed at (+½ θ) ≈ 0.0208º (shift in position), thus the beam divergence angle will deflect to the value equivalent to this response angle.

Case 3: Is a reversed the previous case, where the minimum threshold vibrations at - ½ θ ≈ - 0.020 °, and this attitude is indicated by (C).

The remote side (SCPS-S^{S2}) appears in the right side of the figure18, which shows the status of vibration that, obtains in the FSO-lens system. The results indicated that the diversion angle that was generated via the system's response did not exceed the "maximum acceptance angle" on the receiver's remote side. This indicates that "line of sight" has been achieved between the two systems.

B. System Limitations and the Approach to Avoid Communication Failure

In order to avoid any failure in communication between network nodes, the following method displays proposed scheme in the event of communication failure; in the case of the control system encountering any difficulty to maintain the line of the sight between bi-directional FSO systems. The subsequent method shows the alternative plan to address this failure.

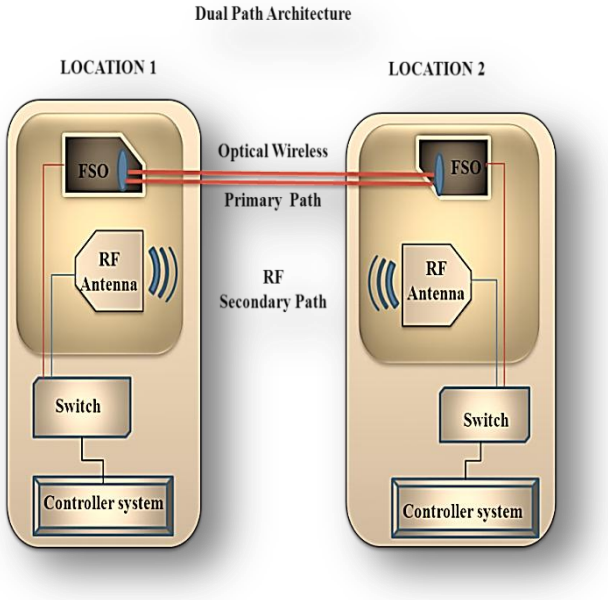

Figure19. Dual-Path Approach between two L-APs

The researchers of [11] studied the distance limitation of FSO systems for both carrier and enterprise applications and showed that carrier class availability can be achieved for much longer link distances if the FSO link is combined with an RF back-up transmitting data redundantly. Hybrid network infrastructures, FSO & RFA approach for point-to-point connectivity consists of three key components (configured as shown in Figure 19), i.e., primary path by means Free-space optical communication, secondary is via (RF) and switching method. The principal of the dual-path approach lies in the failure by a switching mechanism from the primary to the alternative path and vice versa. This approach can be used in the event of failure of the main line to provide the service as a result of external factors such as unstable environmental conditions or other factors. Optical wireless/RF switching algorithm as a back-up is a good approach that can be used in case of failure one of the transmission lines to carry out its functions.

V. CONCLUSIONS

In this research, the feasibility of using LAP-SCPS to enhance communications network in isolated areas has been verified. The obtained results demonstrate the effectiveness of the systems in order to achieve a line of sight between the network nodes as well as examining the performance of an FSO system inter-platform, under different environmental conditions. Multiple laser beam channels have proven its ability to absorb higher attenuation that occurs in the channel transmitter, specifically at less than 1000m altitude. Eventually, these consequences can enhance the functions of information and communication technology proceedings for solving

the bottleneck problem in the "last mile."

ACKNOWLEDGMENT

This research supported by University Malaysia Perlis under grant reference No: RMIC/BEND/01/11(6).

REFERENCES

[1] J. Ure., "Evaluation of the ESCAP subprograms on Information and Communications Technology and Disaster Risk Reduction Consultant's," UN organization, 2012.

[2] Suzuki, H., Kaneko, Y., Mase, K., Yamazaki, S., & Makino, H. (2006). *An Ad Hoc Network in the Sky, SKYMESH, for* Large-Scale Disaster Recovery. Paper presented at the Vehicular Technology Conference, 2006. VTC-2006 Fall. 2006 IEEE 64th

[3] Hariyanto, H.; Santoso, H.; Widiawan, A.K., "Emergency broadband access network using low altitude platform," International Conference on , vol., no., pp.1,6, 23-25 Nov. 2009.

[4] Qiantori, A. (2011). Adoption Of Information And Communication Technology In Indonesia: Focusing On Emergency Medical Communication Systems And Mobile Tv. JP: Acceptance, Graduate School Of Information Systems University Of Electro-Communications.

[5] Alnajjar, S. H., Malek, M. F. A., & Razalli, M. S. (2013). A Novel Approach Evaluation for Enhancing Networks. Procedia Engineering, 53, 497-503.

[6] Alnajjar, S. H., Malek, F., & Wafi, Z. N. K. (2013). Smart Platforms Surveillance System to Enhance Communication in Disaster Environments. International Journal of Engineering and Technology.

[7] Dale E. Seborg, Thomas F. Edgard, Duncan A. Mellichamp, Francis J. Doyle, "Process dynamics and control", Third edition, John Wiley & sons, 2010, pp. 195-502.

[8] Awan, M.S.; Leitgeb, E.; Marzuki; Khan, M.S.; Nadeem, F.;Capsoni, C.; "Evaluation of Fog Attenuation Results for Optical Wireless Links in Free Space," Presented at Satellite and Space Communications,2008.

[9] MRV free-space optics Distribution, Retrieved from http://www.mrvfso.com/TS5000specifications.htm

[10] B. Wandernoth, "5 Photon/bit low complexity 2MBit/s PSK transmission breadboard experiment with homodyne receiver applying synchronization bits and convolutional coding", ECOC '94, 20th European Conference on Optical Communications, Firenze, Sep. 1994.

[11] Kim, I. I., & Korevaar, E. J. (2001, November). Availability of free-space optics (FSO) and hybrid FSO/RF systems. In ITCom 2001: International Symposium on the Convergence of IT and Communications (pp. 84-95). International Society for Optics and Photonics.